Surface Science 606 (2012) 919–923

Contents lists available at SciVerse ScienceDirect

Surface Science

journal homepage: www.elsevier.com/locate/susc

Atomic structure of two-dimensional binary surface alloys: Si(111)-√21×√21 superstructure

Y. Fukaya [a,*], I. Matsuda [b], M. Hashimoto [a], K. Kubo [c], T. Hirahara [c], S. Yamazaki [c], W.H. Choi [d], H.W. Yeom [d], S. Hasegawa [c], A. Kawasuso [a], A. Ichimiya [a]

[a] Advanced Science Research Center, Japan Atomic Energy Agency, 1233 Watanuki, Takasaki, Gunma 370-1292, Japan
[b] ISSP, University of Tokyo, 5-1-5, Kashiwanoha, Kashiwa, Chiba 277-8581, Japan
[c] Department of Physics, University of Tokyo, 7-3-1 Hongo, Bunkyo-ku, Tokyo 113-0033, Japan
[d] Department of Physics and Center for Atomic Wires and Layers, Pohang University of Science and Technology, Pohang 790-784, Republic of Korea

ARTICLE INFO

Article history:
Received 24 May 2011
Accepted 6 February 2012
Available online 19 February 2012

Keywords:
Two-dimensional alloys
Silicon
Gold
Silver
Surface structure
Reflection high-energy positron diffraction (RHEPD)
Photoemission spectroscopy (PES)

ABSTRACT

The atomic structures of Au and Ag co-adsorption-induced √21×√21 superstructure on a Si(111) surface, i.e., (Si(111)-√21×√21-(Au, Ag)), where the Si(111)-5×2-Au surface is used as a substrate, have been investigated using reflection high-energy positron diffraction (RHEPD) and photoemission spectroscopy. From core-level spectra, we determined the chemical environments of Ag and Au atoms present in the Si(111)-√21×√21-(Au, Ag) surface. From the rocking curve and pattern analyses of RHEPD, we found that the atomic coordinates of the Au and Ag atoms were approximately the same as those of the Au and Ag atoms in other Si(111)-√21×√21 surfaces with different stoichiometries. On the basis of the core-level and RHEPD results, we revealed the atomic structure of the Si(111)-√21×√21-(Au, Ag) surface.

1. Introduction

The Si(111)-√3×√3-Ag surface, which is formed by the adsorption of one monolayer (ML) of Ag atoms on a Si(111)-7×7 surface, has been extensively studied as a prototype of a two-dimensional metallic system fabricated on a semiconductor surface [1,2]. In such cases, the coverage, ρ, of 1 ML is defined as 7.83×10^{14} cm^{-2}. The adsorption of noble metal atoms (e.g., Cu, Ag, and Au) on the Si(111)-√3×√3-Ag surface leads to the formation of √21×√21 superstructures. In addition, the surface electrical conductivity sharply increases with increasing coverage of the adsorbed noble metal atoms [1,2]. When the Si(111)-√21×√21 superstructure covers the whole surface, the surface electrical conductivity is maximized. At an additional coverage of 0.14 ML, the conductivity is approximately four times greater than that of a bare Si(111)-√3×√3-Ag surface [1,2]. This drastic increase in electrical conductivity originates from the doping of electrons into the Si(111)-√3×√3-Ag surface since the Fermi circle of the two-dimensional free-electron-like surface state on this surface is dependent upon the amount of noble metal atoms deposited [3].

Recently, we investigated, by means of reflection high-energy positron diffraction (RHEPD), the structure of the Si(111)-√21×√21 surface with $\rho_{Ag}=1.14$ ML and $\rho_{Au}=0.00$ ML, and $\rho_{Ag}=1.00$ ML and $\rho_{Au}=0.14$ ML, where the Si(111)-√3×√3-Ag surface is used as a substrate [4,5]. Although various structural models were proposed by different surface techniques [6–12], we found that the atomic structures for the Si(111)-√21×√21 family are almost identical, save for the marginal difference in adatom heights.

Since the number of valence electrons per atom (e/a) of Ag or Au is equal to 1, formation of the √21×√21 phase is achieved when the total metal coverage is 1.14 ML and e/a is constant. Such one-to-one correspondence between the crystal periodicity and e/a is known to exist in electron compounds in a bulk binary system [13–16]. Therefore, the Ag- and Au-induced Si(111)-√21×√21 superstructure is considered to be a promising candidate as a two-dimensional electron compound, and it has recently been modeled semi-empirically [17]. If the Si(111)-√21×√21 superstructures can be categorized as electron compounds, then Si(111)-√21×√21 superstructures fabricated with different Ag and Au atom stoichiometries will likely have the same structure. In fact, the adsorption of Ag atoms ($\rho_{Ag}=0.74$ ML) on the Si(111)-5×2-Au surface ($\rho_{Au}=0.4$ ML) also results in √21×√21 periodicity [Si(111)-√21×√21-(Au, Ag) surface] in the diffraction pattern [17,18]. In a previous paper [18], we analyzed the profiles of the rocking curves and the intensity distribution in the diffraction

* Corresponding author: Tel.: +81 27 346 9330; fax: +81 27 346 9432.
E-mail address: fukaya.yuki99@jaea.go.jp (Y. Fukaya).

0039-6028/$ – see front matter © 2012 Elsevier B.V. All rights reserved.
doi:10.1016/j.susc.2012.02.006

pattern by substituting the Au atoms with Ag atoms, i.e., all the atoms were assumed to be Ag atoms. Thus, the distinguishing adsorption sites of the Ag and Au atoms in the $\sqrt{21}\times\sqrt{21}$ structure still remain unresolved. In this paper, we find, from core-level photoemission measurements, that Ag and Au atoms individually occupy single chemical sites in the $\sqrt{21}\times\sqrt{21}$-structure. We also re-examine possible structural models by using the RHEPD analysis. The $\sqrt{21}\times\sqrt{21}$-phase, prepared with a different composition of Ag and Au, shows an atomic structure similar to that previously observed, and it can be considered as a regular alloy-type two-dimensional electron compound.

2. Experimental procedure

Substrates were cut from a mirror-polished *n*-type Si(111) wafer with a resistivity of 1–10 Ω·cm. In order to prepare clean 7×7 surfaces, the substrates were annealed at 400 °C for several hours and heated several times at 1200 °C for a few seconds under ultra-high vacuum (UHV) conditions. Then, 0.40 ± 0.08 ML of Au atoms was deposited onto the Si(111)-7×7 surfaces at 600 °C to form a 5×2-Au surface. Finally, 0.74 ± 0.10 ML of Ag atoms was deposited onto the Si(111)-5×2-Au surface at 460 °C. The deposition rates of Ag and Au atoms were calibrated by the formations of Si(111)-$\sqrt{3}\times\sqrt{3}$-Ag and Si(111)-β-$\sqrt{3}\times\sqrt{3}$-Au surfaces, respectively. After the substrate temperature was decreased to room temperature, well-ordered Si(111)-$\sqrt{21}\times\sqrt{21}$-(Au, Ag) surfaces were observed.

The experiments were carried out in two different UHV chambers. The RHEPD measurements were conducted using a highly parallel and well-focused positron beam generated from a ^{22}Na positron source and electromagnetic lens system [19]. The positron beam energy was set at 10 keV. The diffraction patterns were magnified with a microchannel plate and a phosphor screen, and recorded with a charge-coupled-device camera. For the rocking curve measurements, the glancing angle of the incident positron beam was altered by rotating the sample from 0.3° to 6.0°, in steps of 0.1°. Core-level photoemission spectra were recorded with linearly polarized synchrotron radiation on beamline BL-8A1 at Pohang Light Source (Korea). The well-ordered Si(111)-$\sqrt{21}\times\sqrt{21}$-(Au, Ag) surfaces were characterized by low-energy electron diffraction (or reflection high-energy electron diffraction) in the core-level measurements.

3. Results and discussion

Fig. 1(a) shows Ag 4*d* and Au 5*d* spectra for the Si(111)-$\sqrt{3}\times\sqrt{3}$-Ag and Si(111)-$\sqrt{21}\times\sqrt{21}$-(Au, Ag) surfaces. The Ag 4*d* spectrum for the Si(111)-$\sqrt{3}\times\sqrt{3}$-Ag surface has two peaks at a binding energy of around 6 eV. The spectrum is similar to that observed in a previous study [20]. As regards the Si(111)-$\sqrt{21}\times\sqrt{21}$-(Au, Ag) surface, there are two components: Au 5*d* and Ag 4*d*, as shown in Fig. 1(a). This clearly indicates that the Si(111)-$\sqrt{21}\times\sqrt{21}$-(Au, Ag) surface includes both Ag and Au atoms.

Fig. 1(b) shows the Ag 3*d* spectra for the Si(111)-$\sqrt{21}\times\sqrt{21}$-(Au, Ag) and Si(111)-$\sqrt{3}\times\sqrt{3}$-Ag surfaces, and Fig. 1(c) shows the Au 4*f* spectrum for the Si(111)-$\sqrt{21}\times\sqrt{21}$-(Au, Ag) surface. The Ag 3*d* spectrum for the Si(111)-$\sqrt{21}\times\sqrt{21}$-(Au, Ag) surface is very similar to that for the Si(111)-$\sqrt{3}\times\sqrt{3}$-Ag surface, as shown in Fig. 1(b). Since the Ag atoms in the Si(111)-$\sqrt{3}\times\sqrt{3}$-Ag surface are located at the same sites on the surface, those in the Si(111)-$\sqrt{21}\times\sqrt{21}$-(Au, Ag) surface likely take rather identical chemical environment. In fact, each peak can be fitted by a single Voigt function with a spin–orbit splitting of 6.0 eV, as illustrated by the solid lines in Fig. 1(b). In the fitting procedure, the full width at half maximum of the Lorentzian function was fixed at 0.27 eV, as determined in a previous photoemission experiment [21], and that of the Gaussian function was set as a fitting parameter. The Gaussian widths for the Si(111)-$\sqrt{21}\times\sqrt{21}$-(Au, Ag) and Si(111)-$\sqrt{3}\times\sqrt{3}$-Ag surfaces were determined to be 0.37 and 0.44 eV, respectively. With regard to the Au 4*f* spectrum (Fig. 1(c)), we can identify

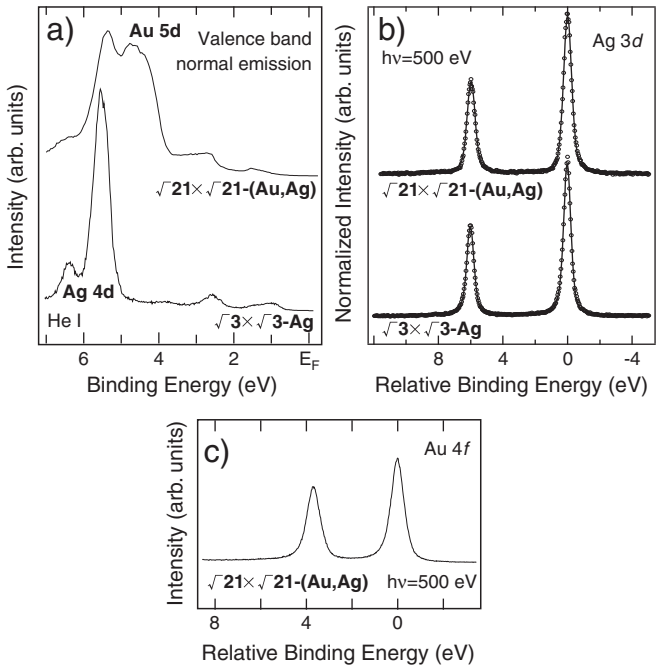

Fig. 1. Core-level spectra of (a) Ag 4*d* for the Si(111)-$\sqrt{3}\times\sqrt{3}$-Ag surface and Au 5*d* for the Si(111)-$\sqrt{21}\times\sqrt{21}$-(Au, Ag) surface, (b) Ag 3*d* for the Si(111)-$\sqrt{3}\times\sqrt{3}$-Ag and Si(111)-$\sqrt{21}\times\sqrt{21}$-(Au, Ag) surfaces, and (c) Au 4*f* for the Si(111)-$\sqrt{21}\times\sqrt{21}$-(Au, Ag) surface. The Ag 4*d*, Ag 3*d*, and Au 4*f* spectra were obtained with a He Iα source and at a photon energy ($h\nu$) of 500 eV, respectively. In (b), the open circles and solid lines denote the experimental and fitted curves, respectively.

two peaks with a spin–orbit splitting of about 3.7 eV [22]. Similarly, each peak in the Au 4*f* spectrum can be reproduced by a single Voigt function. A single Au 4*f* peak with the spin–orbit splitting in the spectrum indicates that the chemical environment of all Au atoms in the Si(111)-$\sqrt{21}\times\sqrt{21}$-(Au, Ag) surface is the same.

The bottom curve in Fig. 2 shows the RHEPD rocking curve for the Si(111)-$\sqrt{21}\times\sqrt{21}$-(Au, Ag) surface at room temperature under a one-beam condition [18]. Under this condition, the RHEPD intensity is very sensitive to the surface-normal components of atomic positions [23]. The rocking curve for the Si(111)-$\sqrt{21}\times\sqrt{21}$-(Au, Ag) surface mainly consists of intense total reflection [24,25] and (111) Bragg reflection. A comparison between the rocking curves for the Si(111)-$\sqrt{21}\times\sqrt{21}$-(Au, Ag) and other Si(111)-$\sqrt{21}\times\sqrt{21}$ surfaces with a different stoichiometry [4,5] shows that the shapes of these curves are similar to each other. This result suggests that there is a similarity in the stacking of Ag and Au atoms in the other Si(111)-$\sqrt{21}\times\sqrt{21}$ and the Si(111)-$\sqrt{21}\times\sqrt{21}$-(Au, Ag) surfaces.

Analyses of the rocking curves at various azimuths were carried out by simulating possible structural models using dynamical diffraction theory [26]. In the atomic model of Fig. 3, for coverage of $\rho_{Ag}=0.74$ ML ($\rho_{Au}=0.4$ ML), there are 24 atomic sites and 15 Ag (9 Au) atoms in the $\sqrt{21}\times\sqrt{21}$ unit cell. Since this results in a million possible Ag and Au combinations, the possible structure models are narrowed down based upon the photoemission results that were recorded before the RHEPD analyses. The adsorption sites for Ag and Au atoms are considered as follows: three adatoms, nine atoms bonded to the adatoms, nine nearest neighbor atoms to the atoms bonded to the adatoms, and the remaining three atoms forming a small triangle (Fig. 3). In fact, there are four different adsorption sites for Ag and Au atoms. On the other hand, the core-level results (Fig. 1) indicate that both the Ag and Au atoms individually have similar chemical environments. To relate the adsorption sites to the chemical environments in the surface structure, Fig. 3 depicts the atomic structural model with chemical bonds (shown as lines in Fig. 3). Subsequently, the metal atoms can be classified into two

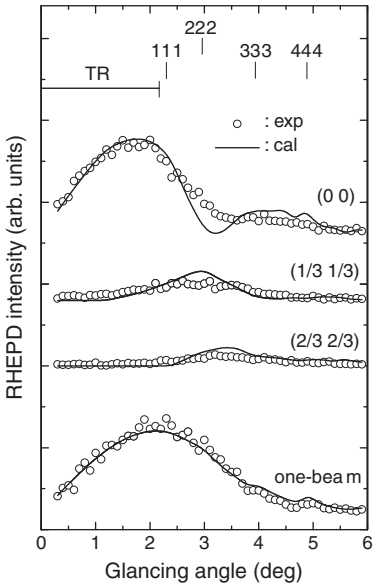

Fig. 2. (Bottom) RHEPD rocking curves of the specular spots for the Si(111)-$\sqrt{21}\times\sqrt{21}$-(Au, Ag) surface at room temperature under the one-beam condition (7.5° away from the [11$\bar{2}$] direction). (Upper) RHEPD rocking curves of the (0 0), (1/3 1/3), and (2/3 2/3) spots for the Si(111)-$\sqrt{21}\times\sqrt{21}$-(Au, Ag) surface at room temperature. The incident azimuth corresponds to the [11$\bar{2}$] direction. The circles indicate the experimental curves [18]. The solid lines show the calculated curves obtained using the optimum parameters. TR stands for the total reflection region.

groups, one that forms a bond with the Si atoms and the other that forms bonds with the Si and the other metal atoms. The chemical environment of an atom is essentially determined by the difference between the electronegativities of the bonding atoms. The electronegativities (χ) of Ag and Si atoms are both 1.9, while that of Au atoms is 2.4 [27]. Therefore, Ag atoms within the Ag – Ag and Ag – Si bonds possess similar chemical characteristics but those within the Au – Ag bond are distinctive. Thus, from stoichiometric considerations based on the chemical properties, the fifteen Ag atoms in the unit cell will likely be distributed as three adatoms, nine atoms that form bonds with the adatoms, and three atoms that compose a small triangle. The Ag atoms are shown as red circles in Fig. 3. On the other hand, the nine Au atoms seem to only occupy the nine Au – Si bonding sites in the cell, as shown by purple circles in Fig. 3. These assignments naturally explain the single-peak (the single chemical environment) of the Ag 3*d* and Au 4*f* spectra (Fig. 1). In the following discussion, structural arguments are made based on this model.

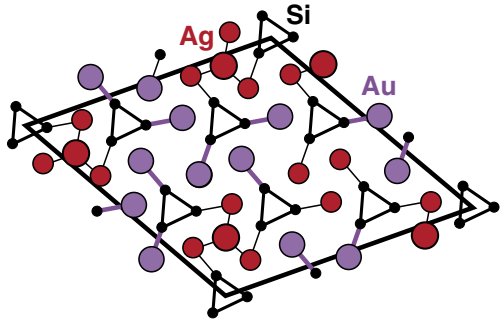

Fig. 3. Ball and stick model of the Si(111)-$\sqrt{21}\times\sqrt{21}$ superstructure. Large and medium-sized red circles indicate the Ag adatoms and the Ag atoms bonded to the adatoms, respectively. Purple circles show the Au atoms and small black circles denote the Si atoms. Gray lines show the Ag – Ag and Ag – Si bonds. Purple and black lines indicate the Au – Si and Si – Si bonds, respectively. The parallelogram denotes the $\sqrt{21}\times\sqrt{21}$ unit cell.

In the calculations performed, the thermal vibrational amplitudes of the Ag and Au atoms, and the Si atoms were assumed to be 0.14 Å and 0.07 Å, respectively [4]. The absorption potentials for the Ag and Au layers, and the Si layer due to electronic excitations (such as single-electron and plasmons) were taken to be 0 eV and 1.70 eV, respectively [4,28]. The atomic coordinates in the binary layer, which was composed of the Ag and Au atoms, were set at the inequivalent triangle (IET) configurations produced by the first-principles calculations [29]. The adatom heights of the Ag atoms were altered so as to provide a fit between the calculated and measured curves. The goodness of fit was justified using the reliability (*R*)-factor [30].

Fig. 4 shows the *R*-factor as a function of the adatom height from the top layer of the underlying IET structure. The value of the *R*-factor has a large dependence on the adatom height. From the minimum *R*-factor, we obtained the optimum adatom height as 0.51 Å from the top layer of the IET structure. The solid line (bottom) in Fig. 2 shows the curve calculated using the optimum adatom height. It should be noted that under the one-beam condition the calculated rocking curve does not vary according to the atomic species composed within the IET structure because the number densities of the Ag and Au atoms in the plane remain constant. The calculated curve is in good agreement with the measured one ($R=1.7\%$). The optimum adatom height of 0.51 Å is similar to that in a previous study concerning the Si(111)-$\sqrt{21}\times\sqrt{21}$ surface with different stoichiometries of Au and Ag atoms [4,5]. Compared with recent first-principles calculation results [11,12], the tendency for the immersion of an adatom into the IET structure is consistent with our result. However, the adatom height obtained in this study is slightly higher than the first-principles calculations.

In order to investigate the atomic configurations in the plane, we measured the RHEPD rocking curves at symmetric azimuths. The open circles (upper) in Fig. 2 show the RHEPD rocking curves for the Si(111)-$\sqrt{21}\times\sqrt{21}$-(Au, Ag) surface along the [11$\bar{2}$] direction [18]. Compared with the previous study on the Si(111)-$\sqrt{21}\times\sqrt{21}$ surface with different stoichiometries of Au and Ag atoms [4,5], we can see that the shapes of the curves for the Si(111)-$\sqrt{21}\times\sqrt{21}$-(Au, Ag) surface along the [11$\bar{2}$] direction are very similar. Again, this result suggests that there is a similarity in atomic coordinates for the Ag and Au atoms on the other Si(111)-$\sqrt{21}\times\sqrt{21}$ and Si(111)-$\sqrt{21}\times\sqrt{21}$-(Au, Ag) surfaces.

We calculated the rocking curves along the [11$\bar{2}$] direction in order to determine the atomic configurations in the plane. The adatom height of the Ag atoms from the top layer of the underlying IET structure was taken to be 0.51 Å, as determined above. In the rocking curve analyses, three different adsorption sites were taken into consideration, namely,

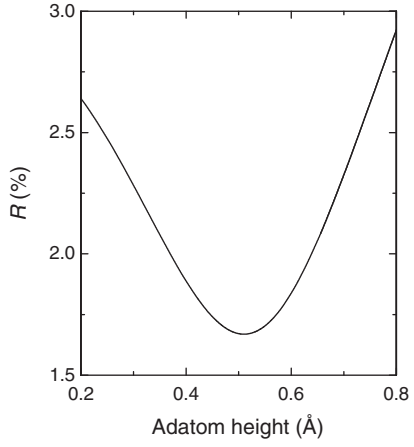

Fig. 4. *R*-factor between the experimental and calculated rocking curves under the one-beam condition as a function of the adatom height. The origin of the adatom height corresponds to the top layer of the underlying IET structure.

at the center of the large triangle, the center of the small triangle, and the center of the Si trimer. As mentioned above, the nine atoms bonded to the adatoms are occupied with Ag atoms (denoted as medium-sized red circles in Fig. 3). As listed in Table 1, when all the adatoms sit at the center of the large triangle in the IET structure, the value of R shows a minimum and the measured curves can be well reproduced by calculation, as shown in Fig. 2 ($R = 2.8\%$). We also calculated the rocking curves when nine Au atoms were bonded to the adatoms. As a result, we found that, in this condition, the differences in the calculated rocking curves for the (0 0), (1/3 1/3), and (2/3 2/3) spots between the atomic species composed of the IET structure are very small. Furthermore, we also found that in this condition, the rocking curves for the (0 0), (1/3 1/3), and (2/3 2/3) spots are not sensitive to the atomic configurations at the center of the large triangle. In order to confirm the in-plane atomic configurations of adatoms and Au atoms in the IET structure, we investigated the line profile of the intensity distribution in the fractional-order Laue zone.

The open circles in Fig. 5 show the experimental profile of the 1/7th Laue zone for the Si(111)-$\sqrt{21}\times\sqrt{21}$-(Au, Ag) surface at room temperature [18]. In the measured line profile, the peak height of the (20/21 17/21) spot is greater than that of the (13/21 10/21) spot. The relation between the peak heights is important for the determination of the adsorption sites of the adatoms [4,5]. The intensity distribution in the 1/7th Laue zone for the Si(111)-$\sqrt{21}\times\sqrt{21}$-(Au, Ag) surface is also approximately the same as those from the other Si(111)-$\sqrt{21}\times\sqrt{21}$ surfaces with different stoichiometries [4,5].

From previous STM observations [16], the atomic configuration of adatoms possesses three-fold rotational symmetry. Thus, there are two possible atomic configurations in which the three adatoms can occupy the center of the large triangles in the IET structure, i.e., the three adatoms either surround the Si trimer or the small triangle in the IET structure. The solid lines (a) and (b) in Fig. 5 represent the line profiles calculated using the structural models with two different atomic configurations. We also calculated the line profiles using the structural models where the nine atoms bonded to the adatoms are occupied by Au atoms, as shown by the solid lines (c) and (d) in Fig. 5. Only the line profile calculated using the structural model of Fig. 3 is able to reproduce the observed relationship between peak heights of the (20/21 17/21) and (13/21 10/21) spots. The observed feature cannot be explained by considering other adsorption sites and atomic species, as shown in Fig. 5. Consequently, we found that the surface structure of Si(111)-$\sqrt{21}\times\sqrt{21}$-(Au, Ag) was very close to that of the other Si(111)-$\sqrt{21}\times\sqrt{21}$ structures with different stoichiometries of Au and Ag atoms.

Based on the present structural model of the Si(111)-$\sqrt{21}\times\sqrt{21}$-(Au, Ag) surface, the bond length between an Ag adatom and the underlying Ag atoms is estimated to be 2.33 Å. The bond length is much shorter than that expected from the atomic radius (2.88 Å). Considering the ionic bonding, the bond length is 2.00–2.56 Å, which is in good agreement with the present value. Therefore, the bond length between the Ag adatom and the underlying Ag atoms in the present model can be explained by considering the ionic bonding that is present in the system.

The topmost layer of the Si(111)-$\sqrt{21}\times\sqrt{21}$-(Au, Ag) surface is composed of the alloys of Au and Ag atoms. Moreover, the Au and Ag atoms within the topmost layer show solid solubility. In this system, therefore, the number of valence electrons per atom plays an important role in the formation of the Si(111)-$\sqrt{21}\times\sqrt{21}$ superstructure. As a result, the Ag- and Au-induced $\sqrt{21}\times\sqrt{21}$ system is consistent with two-dimensional electron compounds. In most cases of bulk binary systems, each atom composed of the alloys is randomly situated at the lattice sites. In other words, with regard to each atom, there is no periodicity in its unit cell. Hence, from the RHEPD analyses using the core-level results, it is inferred that the Si(111)-$\sqrt{21}\times\sqrt{21}$-(Au, Ag) surface is the regular alloy phase.

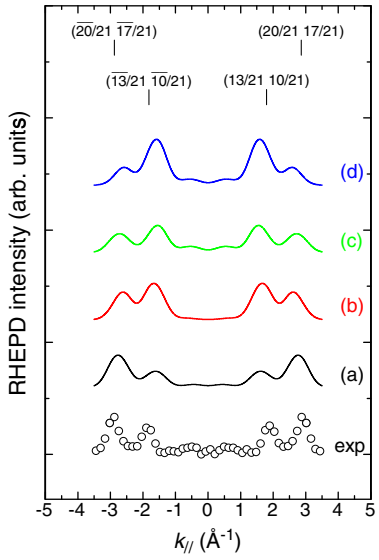

Fig. 5. (Bottom) Line profile of the intensity distribution in the 1/7th Laue zone of the RHEPD pattern measured for the Si(111)-$\sqrt{21}\times\sqrt{21}$-(Au, Ag) surface [18]. (Upper) Calculated line profiles using the structural models where (a) the adatoms surround the Si trimer and the Ag atoms are bonded to the adatoms, (b) the adatoms surround the small triangle and the Ag atoms are bonded to the adatoms, (c) the adatoms surround the Si trimer and the Au atoms are bonded to the adatoms, and (d) the adatoms surround the small triangle and the Au atoms are bonded to the adatoms.

Table 1
R-factors between experimental RHEPD rocking curves and calculated rocking curves for the (0 0), (1/3 1/3), and (2/3 2/3) spots for three adatoms in the unit cell that are individually located at various adsorption sites (center of the large triangle, center of the small triangle, and center of the Si trimer in the IET structure).

Structural model	1	2	3	4	5	6	7	8	9	10
Large triangle	3	2	2	1	1	1	0	0	0	0
Small triangle	0	1	0	2	1	0	3	2	1	0
Si trimer	0	0	1	0	1	2	0	1	2	3
R-factor (%)	2.84	3.52	3.28	4.56	3.29	3.54	6.72	5.12	4.00	3.43

4. Summary

In summary, we investigated the two-dimensional $\sqrt{21}\times\sqrt{21}$ phase composed of Au and Ag atoms, fabricated on a Si(111)-5×2-Au surface. The atomic positions of the Au and Ag atoms in the Si(111)-$\sqrt{21}\times\sqrt{21}$-(Au, Ag) surface are very similar to those in the Si(111)-$\sqrt{21}\times\sqrt{21}$ surfaces having different stoichiometries of Au and Ag atoms.

Acknowledgments

Useful comments on this paper provided by F. Nakamura and H. Narita are gratefully acknowledged. WHC and HWY are supported by CRi program of MEST, Korea. The present work was partly supported by Grant-in-Aid for Young Scientists (B) 22740205 from JSPS.

References

[1] S. Hasegawa, X. Tong, S. Takeda, N. Sato, T. Nagao, Prog. Surf. Sci. 60 (1999) 89.
[2] S. Hasegawa, J. Phys.: Condens. Matter 12 (2000) R463.
[3] J.N. Crain, K.N. Altmann, C. Bromberger, F.J. Himpsel, Phys. Rev. B 66 (2002) 205302.
[4] Y. Fukaya, A. Kawasuso, A. Ichimiya, Surf. Sci. 600 (2006) 3141.
[5] Y. Fukaya, A. Kawasuso, A. Ichimiya, Surf. Sci. 601 (2007) 5187.
[6] J. Nogami, K.J. Wan, X.F. Lin, Surf. Sci. 306 (1994) 81.
[7] A. Ichimiya, H. Nomura, Y. Horio, T. Sato, T. Sueyoshi, M. Iwatsuki, Surf. Rev. Lett. 1 (1994) 1.
[8] X. Tong, Y. Sugiura, T. Nagao, T. Takami, S. Takeda, S. Ino, S. Hasegawa, Surf. Sci. 408 (1998) 146.
[9] H. Tajiri, K. Sumitani, W. Yashiro, S. Nakatani, T. Takahashi, K. Akimoto, H. Sugiyama, X. Zhang, H. Kawata, Surf. Sci. 493 (2001) 214.

[10] C. Liu, I. Matsuda, M. D'angelo, S. Hasegawa, J. Okabayashi, S. Toyoda, M. Oshima, Phys. Rev. B 74 (2006) 235420.
[11] H. Jeong, H.W. Yeom, S. Jeong, Phys. Rev. B 76 (2007) 085423.
[12] X. Xie, J.M. Li, W.G. Chen, F. Wang, S.F. Li, Q. Sun, Y. Jia, J. Phys.: Condens. Matter 22 (2010) 085001.
[13] W. Hume-Rothery, R.E. Smallman, C.W. Haworth, The Structure of Metals and Alloys, The Metals and Metalurgy Trust, London, 1969.
[14] C. Kittel, Introduction to Solid State Physics, John Wiley & Sons, 1997.
[15] T.B. Massalski, U. Mizutani, Prog. Mater. Sci. 22 (1978) 151.
[16] G. Trambly de Laissardière, D. Nguyen-Manh, D. Mayou, Prog. Mater. Sci. 50 (2005) 679.
[17] I. Matsuda, F. Nakamura, K. Kubo, T. Hirahara, S. Yamazaki, W.H. Choi, H.W. Yeom, H. Narita, Y. Fukaya, M. Hashimoto, A. Kawasuso, M. Ono, Y. Hasegawa, S. Hasegawa, K. Kobayashi, Phys. Rev. B 82 (2010) 165330.
[18] Y. Fukaya, I. Matsuda, M. Hashimoto, H. Narita, A. Kawasuso, A. Ichimiya, e-J. Surf. Sci. Nanotechnol. 7 (2009) 432.
[19] A. Kawasuso, T. Ishimoto, M. Maekawa, Y. Fukaya, K. Hayashi, A. Ichimiya, Rev. Sci. Instrum. 75 (2004) 4585.
[20] M. Konishi, I. Matsuda, C. Liu, H. Morikawa, S. Hasegawa, e-J. Surf. Sci. Nanotechnol. 3 (2005) 107.
[21] S. Günther, A. Kolmakov, J. Kovac, M. Marsi, M. Kiskinova, Phys. Rev. B 56 (1997) 5003.
[22] C. Liu, I. Matsuda, T. Hirahara, S. Hasegawa, J. Okabayashi, S. Toyoda, M. Oshima, Surf. Sci. 602 (2008) 3316.
[23] A. Ichimiya, Surf. Sci. 192 (1987) L893.
[24] A. Ichimiya, Solid State Phenom. 28 & 29 (1992/93) 143.
[25] A. Kawasuso, S. Okada, Phys. Rev. Lett. 81 (1998) 2695.
[26] A. Ichimiya, Jpn. J. Appl. Phys., Part 1 22 (1983) 176.
[27] D.R. Lide, CRC Handbook of Chemistry and Physics, 2002–2003: A Ready-Reference Book of Chemical and Physical Data (CRC Handbook of Chemistry and Physics), 83rd ed. CRC, Boca Raton, 2002.
[28] G. Radi, Acta Crystallogr. 26 (1970) 41.
[29] H. Aizawa, M. Tsukada, N. Sato, S. Hasegawa, Surf. Sci. 429 (1999) L509.
[30] Y. Fukaya, A. Kawasuso, K. Hayashi, A. Ichimiya, Phys. Rev. B 70 (2004) 245422.